Quantum well width and barrier thickness effects on the perpendicular transport in polar and non-polar oriented AlGaN/GaN Resonant Tunneling Diodes

Nafaa Kacem, Amel Bhouri, J.-L. Lazzari, Nejeh Jaba

Quantum well width and barrier Thickness effects on the perpendicular transport in polar and non-polar oriented AlGaN/GaN Resonant Tunneling Diodes

Nafaa Kacem
Electronics and Microelectronics Laboratory
Faculty of Sciences of Monastir, University of Monastir
Tunisia,Monastir
nafaakacem@fsm.u-monastir.tn

Amel Bhouri
Electronics and Microelectronics Laboratory
Faculty of Sciences of Monastir, University of Monastir
Tunisia,Monastir
Bhouri_amel@yahoo.fr

Jean-Louis Lazzari
CNRS, CINaM, Case 913, Campus de Luminy
Aix Marseille Univ,
Marseille,France

Nejeh Jaba
Electronics and Microelectronics Laboratory
Faculty of Sciences of Monastir, University of Monastir
Tunisia,Monastir
nejeh.jaba@yahoo.fr

Abstract— **In this study, we theoretically investigated the electronic properties of resonant tunneling diodes (RTDs) grown along the polar and non-polar orientations by using the self-consistent solution of the coupled Schrödinger and Poisson equations. Based on the transfer matrix formalism, the effects of the geometrical parameters on the current-voltage characteristics of $Al_{0.2}Ga_{0.8}N$/GaN RTDs we analyzed by varying GaN well width and $Al_{0.2}Ga_{0.8}N$/GaN barrier thicknesses. The results show that the characteristics of polar and nonpolar $Al_{0.2}Ga_{0.8}$ N/GaN RTD strongly depend on the barrier and well size; showing a strong decrease in peak and valley current density and a large PVR enhancement when increasing well and barrier thickness. To bring interesting RTD electrical characteristics, a comparison between the polar and non-polar $Al_{0.2}$ $Ga_{0.8}N$/GaN RTD was performed. non-polar oriented RTDs show better electronic characteristics, including higher peak current density (*Jpeak*), smaller peak voltage (*V*peak), and greater pic-to-valley ratio (PVR), than polar ones**

Keywords— Nitride semiconductors, Polar and Non-Polar oriented Resonant Tunneling Diodes, Ballistic transport, Peak-to-Valley Ratios)

I. INTRODUCTION

In the last few years, terahertz (THz) emission sources have been the subject of much research thanks to their many applications in various sectors such as information and communication technology [1], radar and security [2], and medical sciences [3]. Resonant tunneling diodes (RTDs), with their high cut-off frequency and excellent output power performance, present a promising candidate for THz sources [4]. Particularly, the THz oscillator, based on gallium nitride (GaN), is considered one of the most efficient electronic devices to date, owing to the excellent properties of GaN [5, 6]. In fact, such properties include wide bandgap energy, high carrier mobility, high electron peak velocity, high thermal stability, and saturation electron velocity. The highest resistive cut-off frequency of an RTD, which is dependent on the peak-to-valley (PVR), is theoretically the maximum operating frequency of the oscillator and represents an advantage of the output power [4]. Therefore, the recent works of GaN-based RTD are mainly focused on raising the peak current, reducing the valley voltage, and enhancing the PVR. Based on the formalism of the transfer matrix, the authors of references [6, 7] investigated the influence of barrier thicknesses and well widths as well as the effect of aluminum

978-0-7381-3264-8/21/$31.00 ©2021 IEEE

concentration on the evolution of the current characteristics and the device performance of GaN-based RTDs. In the same context of improving the electronic properties of RTDs, Rong and al. [8] investigated the influence of growth orientation of AlGaN⁄GaN RTDs on the current-voltage (J–V) characteristics and they proved that the current peak and the PVR of non-polar RTDs AlGaN⁄GaN are higher than polar ones. In this paper, we will use our self-developed code to first simulate the conduction band profile in polar and non-polar $Al_{0.2}Ga_{0.8}N/GaN$-based RTDs. such simulation is done by solving the coupled Schrödinger and Poisson differential self consistently using the finite differential method [9] and taking into account the piezoelectric and spontaneous polarization fields in the case of polar RTDs. Transmission coefficient and tunnel current are calculated through the formalism of the transfer matrix supposing ballistic transport [7].Then we will focus on analyzing and comparing the evolution of the calculated current-voltage (J-V) characteristics, by varying the GaN quantum well width and barrier thickness, for both orientation cases. This work will enable us to improve the performance of the diode such as the peak current, valley current, and PVRs and also to show that the performance enhancement of non-polar RTDs is more obvious than that of polar RTDs

II. THEORETICAL FORMULATION

Numerical modeling of RTD is a practical solution for understanding theory and helping experimenters to analyze their observations. The procedure for calculating the conduction band profile and free-electron distribution is based on solving self-consistently the coupled Schrödinger-Poisson equations along the quantization axis (oz). The Schrödinger equation along the direction of the quantization axis (oz) is as follows:

$$\left[-\frac{\hbar^2}{2}\frac{\partial}{\partial z}\frac{1}{m_e^*(z)}\frac{\partial}{\partial z}+U(z)\right]\varphi_n(z)=E_n\varphi_n(z) \quad (1)$$

with $m_e^*(z)$, $\varphi_n(z)$ and E_n represent the reduced effective electron mass, the wave function, and the energy level of the n^{th} subband, respectively. U(z) is the potential energy of the electron which is expressed as follows:

$$U(z)=\Delta E_c(z)+V_H(z)+V_{ext} \quad (2)$$

with $\Delta E_c(z)$ is the conduction band discontinuity, V_{ext} is the external bias applied to the structure and $V_H(z)$ is the Hartree potential along the z-direction which is determined by solving Poisson's equation:

$$\frac{\partial}{\partial z}\left(-\varepsilon(z)\frac{\partial}{\partial z}V_H(z)+P_{tot}(z)\right)=q\big(N_D(z)-n(z)\big) \quad (3)$$

$N_D(z)$ is the doping concentration, n(z) is free-electron concentration, ε(z) is the dielectric constant along the z-direction, and $P_{tot}(z)$ is the total polarization. Furthermore, it is important to note that the total polarization $P_{tot}(z)$ is the sum of both piezoelectric and spontaneous polarization. However, the total polarization effect in the non-polar orientation is canceled because both the electric field direction and growth plane direction are perpendicular, and then the Poisson equation will be expressed as follows:

$$\frac{\partial}{\partial z}\left(-\varepsilon(z)\frac{\partial}{\partial z}V_H(z)\right)=q\big(N_D(z)-n(z)\big) \quad (4)$$

To calculate the Hartree potential $V_H(z)$, Poisson's equation is solved from an initial estimated value of the charge density $n_{essai}^0(z)$, and then it is inserted into equation(1) to obtain the energy levels E_n and the wave functions φ_n of the simulated system. Afterward, these eigenstates and wave functions are utilized in the calculation of the new electron charge density through the total electron concentration which is given as follows:

$$n(z)=\sum_n n_n\left|\varphi_{n,k_z}(z)\right|^2 \quad (5)$$

$$n_n=\frac{m_e^* k_B T}{\pi\hbar^2}\log\left[1+\exp\frac{E_f-E_n}{k_B T}\right] \quad (6)$$

where k_B is Boltzmann's constant and E_f is the Fermi level In the last few years, theorists have proposed several approaches to model the tunneling current density J–V, most notably the approximation of Wentzel-Kramers-Brillouin (WKB)[10], the Green's function[11], and the transfer matrix formalisms[6, 7]. In this paper, we have adopted the formalism of the transfer matrix, which is appropriate for the

treatment of any arbitrary potential energy profile. This method is based on the discretization of the energy potential $V_H(z)$ into small sections of potentiel $V_{H_i}(z_i)$. For a discretized section i, the wave function in-plane wave form is expressed by:

$$\varphi_i(z_i) = A_i e^{(jk_i z_i)} + B_i e^{(-jk_i z_i)} \quad (7)$$

with A_i and B_i representing the transmission and reflection coefficients respectively and $k_i = \sqrt{\frac{2m_i(E-V_i)}{\hbar^2}}$ is the wave vector. A_i and B_i are found by matching φ and $\frac{1}{m_i}\frac{\partial \varphi_i}{\partial z_i}$ at each i interface, Therefore, the wave coefficients for two consecutive meshes i and i+1 can be related to the transfer matrix as below:

$$\begin{pmatrix} A_{i+1} \\ B_{i+1} \end{pmatrix} = M_i \begin{pmatrix} A_i \\ B_i \end{pmatrix} \quad (8)$$

$$M_i = \frac{1}{2}\begin{pmatrix} \left(1+\frac{m_{i+1}}{m_i}\frac{k_i}{k_{i+1}}\right)e^{j(k_i-k_{i+1})z_i} & \left(1-\frac{m_{i+1}}{m_i}\frac{k_i}{k_{i+1}}\right)e^{-j(k_i+k_{i+1})z_i} \\ \left(1-\frac{m_{i+1}}{m_i}\frac{k_i}{k_{i+1}}\right)e^{j(k_i+k_{i+1})z_i} & \left(1+\frac{m_{i+1}}{m_i}\frac{k_i}{k_{i+1}}\right)e^{-j(k_i-k_{i+1})z_i} \end{pmatrix} \quad (9)$$

Using this Transfer matrix, we can calculate the probability of transmission, which is defined as the ratio between the transmitted and incident electron flow:

$$T(E) = \frac{\frac{|A_N|^2 k_N}{m_N}}{\frac{|A_0|^2 k_0}{m_0}} \quad (10)$$

It can be also noted that this transmission probability is determined by a plane-wave function system considering both incidents and reflected waves at each point of a discrete mesh and including the boundary-limiting conditions. Furthermore, according to Tsu-Esaki's formalism[12], the current density can be defined as a function of the applied voltage after the integration in the longitudinal energy:

$$J_T(V_{ext}) = \frac{e\, m_e^* k_B T}{2\pi^2 \hbar^3} \int_0^\infty T(E)\, ln \frac{1+exp\left[\frac{E_f - E}{k_B T}\right]}{1+exp\left[\frac{E_f - E - eV_{ext}}{k_B T}\right]} dE \quad (11)$$

where m_e^*, E_f and V_{ext} represent the reduced electron effective mass, the Fermi energy, and the applied voltage, respectively. Based on the theoretical formalism and the set of equations, detailed above, we will study the mechanism of tunneling transport in polar and non-polar $Al_{0.2}Ga_{0.8}N/GaN$ heterostructures and analyze their dependence on geometrical parameters such as the well width and barrier thickness.

III. Simulation Results

The RTD structure studied is composed of an undoped GaN well bordered by two $Al_{0.2}GaN_{0.8}$ barriers and delimited by undoped GaN layers acting as a spacer. This active region is sandwiched between two n-doped GaN layers ($n = 5 \times 10^{18} cm^{-3}$). The condition band profile of RTD grown along the polar and non-polar orientations is shown in fig.1.

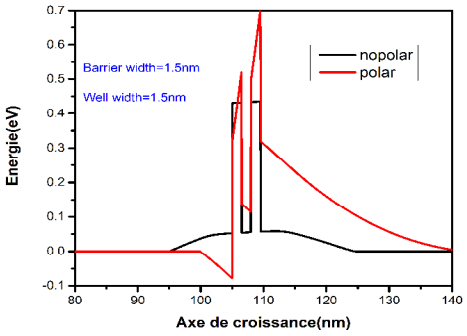

Fig. 1. Figure 1: $Al_{0.2}Ga_{0.8}N/GaN$ conduction band profile in the cases of polar (red lines) and non-polar (black lines) orientation

In the case of nonpolar RTD, this condition band is symmetric and no depletion region is formed. However, the internal polarization which characterizes the polar RTD leads to the formation of a two-dimensional electron gas (2DEG) specified by a shallow triangular well between the left barrier and the emitter, and a depletion region on the right side of the active zone. The influence of this internal polarization is not only limited to the conduction band profile but also affects the RTD's electronic characteristics, such as the current voltage characteristics and the PVRs.

TABLE I. Confined energy level values in the $Al_{0.2}Ga_{0.8}N/GaN$ RTDs for different well widths.

Orientation	***Polar***			***non-polar***		
well width(nm)	1	1.5	2	1	1.5	2
Quasi-Bound State (eV)	0.38	0.35	0.23	0.3	0.25	0.16

The results obtained also show that only one quantum level is confined for both polar and non-polar orientation. Hence, by increasing the GaN well width the quantum level becomes deeper and shifts to the low-energy (table I).

In the following section, we will study the variation of current density versus GaN well width Lw ($1nm \leq L_w \leq 2nm$). The $Al_{0.2}GaN_{0.8}$ barrier thickness is fixed at 1.5 nm. The observation of the $J-V$ characteristics in the polar (fig.2(a)) and nonpolar (fig.2(b)) orientations shows that the resonance peak progressively shifts to a lower voltage as the well width increases. This can be explained by the dependence of the confined quasi-bound state on the well width. In fact, as the well width (Lw) increases, both resonant and Fermi levels become more closely spaced, which requires less external bias to reach resonance. Besides, we note that the intensity of the peak and valley currents corresponding to the non-polar orientation is always greater than that of the polar one.

We can explain the origin of this high peak current density in the non-polar orientation by analyzing the tunnel current density expression that depends on both the electron's effective mass m* [13] and the maximum transmission probability T_{max} [14] :

$$J_{res} \cong \frac{em^*}{2\pi h}.T_{max}.\Delta E.E_f \qquad (12)$$

In fact, the order of magnitude of both the effective electron mass and the maximum transmission coefficient, according to the literature[8], is greater in the nonpolar orientation than in the polar one which explains the increase of peak current. Nevertheless, the reduction in the valley current appears stronger than that of the peak current, resulting in a great enhancement of the PVR values. For example, in polar RTD the PVR value varies from 1.62 for a well width of 1 nm to 2.91 for 2 nm well width. The PVR enhancement is most noticeable in the case of non-polar orientation witch increases from 2.08 for a well width of 1 nm to 4.74 for a well width of 2 nm. The obtained results are summarized in Table II.. These results are consistent with those of the references [6, 15].In fact, the authors of the latter references have shown that the PVR in the current density profile is reduced and the current peak is shifted to a lower bias voltage by increasing the quantum well width for a specified barrier value.

TABLE II. Peak Positions and PVR values as a function of well widths for polar and non-polar orientation $Al_{0.2}Ga_{0.8}N/GaN$ RTDs

Polar orientation					
Well width (nm)	***Peak voltage (V)***	***Valley voltage (V)***	***Peak current density A.cm^{-2}***	***Valley current density A.cm^{-2}***	***PVR***
1	0.94	1.18	40.85×10^5	25.07×10^5	1.62
1.5	0.74	0.94	28.191×10^5	12.63×10^5	2.23
2	0.3	0.5	17.839×10^5	6.126×10^5	2.91
Non-polar orientation					
1	0.28	0.42	42.24×10^5	20.27×10^5	2.08
1.5	0.2	0.34	33.89×10^5	10.24×10^5	3.32
2	0.14	0.26	29.69×10^5	6.25×10^5	4.74

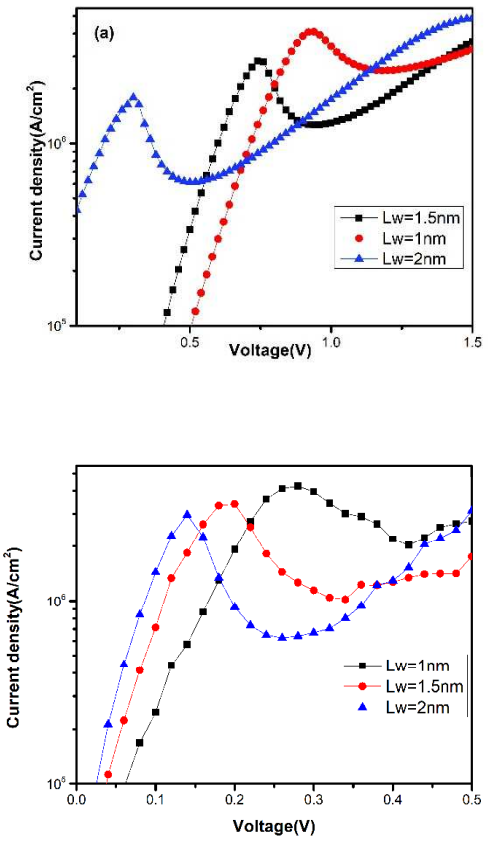

Fig. 2. Variation of (J-V) characteristics in polar (a) and non-polar (b) orientations for different quantum well widths

In the following, we will focus on studying the effect of the barrier thickness on the $J-V$ characteristics, for polar and nonpolar orientation, of the $Al_{0.2}GaN_{0.8}/GaN$ RTDs. At first sight, we notice an obvious curve around 0.8 volts for the polar orientation (fig.3 (a)) and 0.2 volts for the non-polar

orientation (fig.3 (b)). This curve characterizes the negative differential resistance NDR which is one of the most important properties of tunnel diodes and is much more visible in diodes grown along with the non-polar orientation than along the polar orientation. Indeed, when the barrier thickness increases, the resonance, and Fermi levels become more separated, which requires more external polarization to reach the resonance. This explains the difference between the voltage peaks near 0.8 and 0.2 volts for the polar(fig.3 (a)) and nonpolar orientation(fig.3 (a)), respectively. These results are in agreement with those of reference [6]. Indeed Rached and al have shown that for wurtzite $Al_xGa_{1-x}N$/GaN-based RTDs, the valley current decreases with barrier height and width.

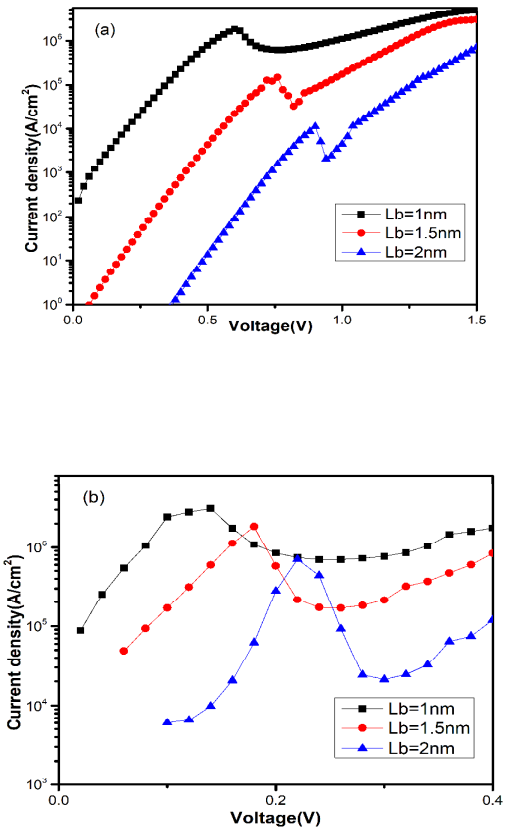

Fig. 3. Variation of (J-V) characteristics in polar (a) and non-polar orientations (b) for different barrier thicknesses

The obtained results are depicted in fig.3 and show similar behavior for both polar (fig3a) and non-polar orientations(fig3b). In fact, the peak and valley current densities decrease as the barrier thickness increases. This phenomenon can be explained as follows: the polarization discontinuity between $Al_{0.2}GaN_{0.8}$ barrier and GaN quantum well become more important as the thickness of the barrier increases. The latter involves the shifting of central QW resonance levels far from the edge of the conduction band and the appearance of a more important depletion region for polar RTDs which leads to a reduction of the resonance intensity peak. The latter reaches a minimum of 0.13×10^5 A. cm^{-2} for a 2 nm barrier thickness and a maximum of 18.23×10^5 A. cm^{-2} for a 1 nm barrier thickness in the case of polar RTDs. This peak current will be more important in the case of non-polar RTDs, ranging from 7.39×10^5 A. cm^{-2} for the 2 nm barrier thickness to 31.1×10^5 A. cm^{-2} for 1 nm (Table III).

TABLE III. Peak Positions and PVR values as a function of barrier thickness for polar and non-polar orientation Al0.2Ga0.8N/GaN RTDs

Polar orientation					
Barrier thickness (nm)	***Peak voltage (V)***	***Valley voltage (V)***	***Peak current density ($A.cm^{-2}$)***	***Valley current density ($A.cm^{-2}$)***	***PVR***
1	0.6	0.76	18.237×10^5	6.221×10^5	2.93
1.5	0.76	0.82	1.484×10^5	0.33×10^5	4.47
2	0.9	0.94	0.1325×10^5	0.02×10^5	5.48
Non-polar orientation					
1	0.14	0.24	31.1×10^5	6.987×10^5	4.45
1.5	0.18	0.26	18.47×10^5	1.678×10^5	11.01
2	0.22	0.3	7.39×10^5	0.211×10^5	34.95

However, the PVR values are highly enhanced as the barrier thickness is increased, since the valley current decreases faster than the peak current. For polar RTD, the PVR increases from 2.93 for a barrier thickness of 1 nm to 5.48 for a barrier thickness of 2 nm, and this increase remains greater for non-polar RTD, which ranges from 4.45 for a barrier thickness of 1 nm to 34.95 a barrier thickness of 2 nm. Besides, the positions of the valley and the peak voltage shift to the high voltage caused by the decrease in the electron probability transmission. This enhancement of PVR in the non-polar orientation and especially at a barrier width of 2 nm may be explained based on the following expression [16]:

$$J = J_{RT} + J_{EX} \qquad (13)$$

where J_{RT} and J_{EX} are the tunneling resonance current and the excess residual current, respectively. The J_{RT} is highly dependent on the peak current, as mentioned above.J_{EX} represents a part of the valley current J_V, and it is also

dominated by thermionic current, that can be determined by the barrier height., The reduction in height of the barrier in the non-polar orientation compared to the polar one can lead to an increase in J_{EX}, thus raising the J_V.

Nevertheless, this decrease in barrier height is much smaller than the effective mass and the transmission coefficient increase. This means that the rise in the peak current is more important than the increase in the valley current which explains the high PVR in the non-polar orientation.

IV. Conclusion

In conclusion, we investigated self-consistently the effects of quantum well width and barrier thickness on the conduction band profile and current-voltage characteristic in polar and non-polar oriented $Al_{0.2}Ga_{0.8}N/GaN$ RTDs.The results revealed, in both polar and nonpolar grown orientations, that decreasing of the well and the barrier width enhances reduces the PVR and increases the peak and valley current density by shifting them towards lower bias voltages. However the non-polar $Al_{0.2}Ga_{0.8}N/GaN$ RTD exhibited an improvement in these electronic characteristics compared to polar $Al_{0.2}Ga_{0.8}N/GaN$ RTD, notably higher peak current density, lower peak voltage, and higher PVR. From our point of view, this work can be very beneficial for designing terahertz devices based on the J−V characteristics of GaN RTDs

References

[1]. Lee, K. and Y. Jeong, *A Compact RTD-Based Push-Push Oscillator Using a Symmetrical Spiral Inductor.* IEICE Transactions on Electronics, 2021. **104**(1): p. 37-39.

[2]. Daneshmandian, F., A. Abdipour, and A. Askarpour, *Numerical modeling of highly sensitive resonant detection of THz radiation using a multichannel dispersive plasmonic HEMT.* Journal of Computational Electronics, 2021: p. 1-10.

[3]. Ouchi, T., et al., *Terahertz imaging system for medical applications and related high efficiency terahertz devices.* Journal of Infrared, Millimeter, and Terahertz Waves, 2014. **35**(1): p. 118-130.

[4]. Gao, B., et al., *Influence of the heterojunction spacer on the performance of AlGaN/GaN/AlGaN resonant tunneling diodes.* IEEE Transactions on Electron Devices, 2016. **64**(1): p. 84-88.

[5]. Lin, S., et al., *III-nitrides based resonant tunneling diodes.* Journal of Physics D: Applied Physics, 2020. **53**(25): p. 253002.

[6]. Rached, A., et al., *Self-consistent vertical transport calculations in AlxGa1–xN/GaN based resonant tunneling diode.* Superlattices and Microstructures, 2016. **91**: p. 37-50.

[7]. Sakr, S., et al., *Ballistic transport in GaN/AlGaN resonant tunneling diodes.* Journal of Applied Physics, 2011. **109**(2): p. 023717.

[8]. Rong, T., et al., *Performance of resonant tunneling diodes based on the nonpolar-oriented AlGaN/GaN heterostructures.* Japanese Journal of Applied Physics, 2018. **57**(7): p. 070303.

[9]. Tan, I.H., et al., *A self‐consistent solution of Schrödinger–Poisson equations using a nonuniform mesh.* Journal of applied physics, 1990. **68**(8): p. 4071-4076.

[10]. Huang, Z., et al., *Wentzel-Kramers-Brillouin method in multidimensional tunneling.* Physical Review A, 1990. **41**(1): p. 32.

[11]. Akdoğan, Z., M. Demirci, and O.S. Mukhtarov, *Green function of discontinuous boundary‐value problem with transmission conditions.* Mathematical Methods in the Applied Sciences, 2007. **30**(14): p. 1719-1738.

[12]. Tsu, R. and L. Esaki, *Tunneling in a finite superlattice.* Applied Physics Letters, 1973. **22**(11): p. 562-564.

[13]. Encomendero, J., et al., *New tunneling features in polar III-nitride resonant tunneling diodes.* Physical Review X, 2017. **7**(4): p. 041017.

[14]. Sun, J.P., et al., *Resonant tunneling diodes: Models and properties.* Proceedings of the IEEE, 1998. **86**(4): p. 641-660.

[15]. Dakhlaoui, H. and S. Almansour, *Piezoelectric polarization and quantum size effects on the vertical transport in AlGaN/GaN resonant tunneling diodes.* Chinese Physics B, 2016. **25**(6): p. 067304.

[16]. Tsuchiya, M. and H. Sakaki, *Precise control of resonant tunneling current in AlAs/GaAs/AlAs double barrier diodes with atomically-controlled barrier widths.* Japanese journal of applied physics, 1986. **25**(3A): p. L185.